

## IMPACT OF END EFFECTOR TECHNOLOGY ON TELEMANIPULATION PERFORMANCE

A. K. Bejczy, Z. Szakaly and T. Ohm  
 Jet Propulsion Laboratory  
 California Institute of Technology  
 Pasadena, California 91109

## ABSTRACT

This paper is subdivided into three parts. In the first part generic requirements for end effector design are briefly summarized as derived from generic functional and operational requirements. Included in this part of the paper is a brief summary of terms and definitions related to end effector technology. The second part of the paper contains a brief overview of end effector technology work as JPL during the past ten years, with emphasis on the evolution of new mechanical, sensing and control capabilities of end effectors. The third and major part of the paper is devoted to the description of current end effector technology work at JPL. The ongoing work addresses mechanical, sensing and control details with emphasis on mechanical ruggedness, increased resolution in sensing, and close electronic and control integration with overall telemanipulator control system.

## INTRODUCTION

Space operations planned in the next decade include assembly, servicing and repair of space systems. Some of these operations are expected to be performed by the use of teleoperators or telerobots. The difference between teleoperator and telerobot is the mode of control. A teleoperator is continuously controlled by a human operator in all activities. In contrast, a robotic system operates in automatic mode of control. A telerobot combines control elements of teleoperators and robots. A telerobot system permits both direct operator control and automatic control supervised by the operator.

The term "telemanipulation" used in the title of this paper signifies a remote manipulator system and its operation in both teleoperator and telerobotic modes of control, including all elements needed for the remote operation: the

arm, hand, sensors, electronics, microprocessor, interfaces, base support, communication links, the control station with displays and with manual and computer control input devices.

Robot hands, or end effectors, are essential elements of telerobot systems to be employed in space since, in the proper sense of the word, "manipulation" is the function of the hand. Using the analogy of the human arm-hand system, the arm is a positioning, orienting, power and information transmission device, while the hand is a powerful tool and delicate sensory organ. Dexterity and smartness in telemanipulation to a large extent resides in the capabilities of robot hands. End effector technology has a major impact on task performance in telemanipulation.

In the first part of the paper generic end effector functional requirements are outlined including terms and definitions. End effector technology work at JPL during the past ten years is briefly reviewed in the second part of the paper. In the third and major part of the paper ongoing end effector technology work at JPL is described.

## REQUIREMENTS, TERMS AND DEFINITIONS

The general hand design requirements can be subdivided into four principal areas: (i) mechanism, (ii) sensing, data acquisition and transmission, (iii) control, and (iv) man-machine interface for decision and control.

## Mechanism

The most important function a hand has to perform is to grasp and to hold objects. Even though this seems to be rather simple, one has to keep in mind that objects come in different sizes, weights and shapes and with many more characteristics to be considered such as fragility, ob-

ject presentation, space restrictions, accuracy, etc.

It is obvious that no single hand design can accommodate all requirements to successfully handle all objects. Even the most sophisticated end effector, the human hand, uses a variety of manual and power tools and still needs other aiding devices for even quite common tasks.

In searching for an answer of what comprises a useful robot hand from a mechanical point of view, the word "versatility" comes to ones mind: if the end effector can handle a large variety of different objects, it can be considered versatile. More sophistication will be gained if the hand is able to manipulate objects (i.e., to turn an object within the hand or pull the trigger of a hand-held drill press while holding it).

Employing tools was the turning point that changed early man's life. It will have the same effect on robot hands where the usage of tools will enhance the robotic capabilities and application ranges. But one hand alone cannot accomplish much by itself. Therefore, the final configuration of a robot hand system will be a multi-handed configuration permitting exchange of end effectors on a given arm.

Two types of hands need to be considered. The first is the one degree of freedom hand which can be made smart through incorporating a variety of different sensing capabilities built into the hand. Its mechanical design is relatively simple, thus reliable. But it is limited to grasping objects without manipulating them. The other type of smart hand is the dexterous hand with several fingers and finger joints. In this paper we only consider one-dimensional robot hands.

One-dimensional hands have to opposing fingers of some geometrical form that can clamp the workpiece in-between. Hand performance requirements for these hands can be established according to the required tasks to be accomplished. The capability to execute as many tasks as possible with one hand design will determine the hand's kinematic motion and shape. Should one hand not cover all intended applications, exchangeable plug-in end effectors might be considered, especially if the objects and loads vary greatly in size and shape.

It is usually desirable to have concave sections in the clamping surfaces to lock-in the object rather than relying on frictional forces alone. Hugging an object allows reduction in clamping force which might result in structural size

reduction. Concave surfaces and other geometrical shapes also assist in grasping and centering of workpiece in the gripping area. It will aid the controller in recognizing if the object is properly grasped. The clamping force should be adjustable.

A linear closing motion is best suited for control purposes. Independent activation of each finger can aid in aligning the hand for grasping. Even better is a coasting capability while grappling so that the fingers can align at the object. Elastic elements or a spring system can be incorporated in the finger, assuring better clamping characteristics with a more gradual force application and reduced slippage between hand and workpiece.

#### Sensors

Intelligent operations require a great amount of sensory information which includes force, moment, position, tactile, temperature and proximity sensing, object recognition, global and local vision and many more. Space permitting, any number of sensors can be built into the hand. Much work is needed to down-scale the sizes of sensors, for most of them are far too bulky for practical applications within or at the hand.

If possible, sensors and feedback routing should be placed entirely within the physical confinements of the hand for protection. Otherwise, contaminants and moisture inflow might hamper their operations or material handling may crush them if located in exposed positions. Tactile and any other sensors which are located on the surface need to be sealed and extremely rugged. The amount of sensory feedback will determine if local pre-processor are needed. Multiplexing will always be necessary with smart hands.

#### Control

Robots do not yet have the capability to adjust to major changing situations. A human operator is therefore required in the control loop to make all major control decisions. Artificial intelligence will eventually help but is still years away in its development. With human operators controlling the teleoperation system, the controller must present the pre-evaluated feedback to the operator in easy-to-understand form for quick recognition, comprehension and decision-making by the operator.

#### Man-Machine Interface

The information flow between the operator and the teleoperator system is a presen-

tation of sensed information to the operator and the operator's control decisions back to the controller.

With vision being the most important sense, a visual signal in the form of a mono or stereo TV picture will have to be transmitted to the operator from the mechanical hand. It will provide the operator with a sense for where the hand is reaching. Additional cameras might be mounted at the arms of the robot to aid in grasping. Other sensory information can be presented in graphic, acoustic or some other form that provides convenient state evaluation possibilities for the operator.

Mechanical, electromechanical and electrical interfaces are common in master-slave arrangements. Positional control will be simplified if the operator manually performs the motion which the end effector will repeat. This positional control can be done in a master-slave control arrangement. The master-slave arrangements incorporate backdriving (or force-reflecting) capability. This capability greatly enhances the operator's perception for control decisions.

General and specific end effector technology requirements are treated in more details in References 1 and 2.

#### PAST END EFFECTOR DEVELOPMENT AT JPL

The JPL end effector development adopted an evolutionary approach to generate important and needed capability increases stepwise. The basic idea was that the first generation smart hand models should be one degree-of-freedom (d.o.f.) parallel-claw end effectors equipped with proximity, tactile, six d.o.f. force-torque and one d.o.f. grasp force sensors. Several smart hands of this category have been developed during the past ten years. These prototype models differ in their end effector size, drive mechanism, claw shapes, load handling capacity, local electronics and control design, and subsystem interface instrumentation.

An early smart hand prototype is shown in Figure 1. Indicated on the figure are three sensors: a six d.o.f. wrist force-torque balance sensor, two proximity sensors in each claw, one pointing forward and one pointing downward, and a thirty-two-point touch sensor on each claw. Each touch-sensing spot in the gripping area is actually a copper pin. The contact pressure on the pin will cause the circuit underneath to close, generating a simple "on" signal. The center-to-center distance between the contact pins determines the touch sensing area resolu-

tion. The proximity sensors in Figure 1 have a distance sensing range of 4 inches with a resolution of 0.05 inches. More on this smart hand can be found in References 3 and 4.

Two smart hands are shown in Figures 2 and 3 developed for control performance evaluation using the simulated Space Shuttle Remote Manipulator System (RMS) at the Johnson Space Center (JSC). The four-claw end effector shown in Figure 2 is equipped with four proximity sensors with a distance sensing range of six inches. These sensors can measure range and pitch and yaw alignment errors. More on this experimental sensor system and on the performance results can be found in Reference 5. The end effector, which can have a four-claw or three-claw configuration and shown in Figure 3 is equipped with a force-torque sensor with a dynamic sensing range of 200 lbs, with 0.2 lbs resolution. The end effector assembly schematic clearly shows that the force-torque sensor frame is an integral part of the end effector mechanism. In fact, the whole mechanism is designed around the sensor frame. Note also in Figure 3 the local electronic instrumentation required to operate this system. More on this smart hand and on the experimental results can be found in References 6 and 7.

Figure 4 shows a smart hand designed for tests on an Orbiting Maneuvering Vehicle (OMV) Protoflight Manipulator Arm (PFMA) at the Marshall Space flight Center (MSFC). The JPL-OMV smart hand is a one-d.o.f. gripper with intermeshing jaws consisting of parallel plates with a V groove center section. Thus, the claws can mechanically lock on square or cylindrical objects in two-d.o.f. The jaws can travel on a linear path while gripping, and their maximum opening at the tip is 6.5 cm. Each jaw has a built-in load cell to measure gripping force in the range of one to 600 Newtons. The jaws are driven by a DC motor via opposing lead screws. Double slides, supported at both ends for compactness and stiffness, guide the jaws' motion. Each slide is on a separate hardened and ground steel rod. A channel built into the drive system's frame gives additional guidance. The entire smart hand mechanism mounts to the robot arm wrist through a six-d.o.f. strain gauge load cell system by which the three interaction forces ( $F_x$ ,  $F_y$ ,  $F_z$ ) and moments ( $M_x$ ,  $M_y$ ,  $M_z$ ) with the environment are measured in the range of 120 Newtons and 70 Newton-Meters.

Self contained in sensor data acquisition, data processing and motor control, the JPL-OMV smart hand has three built-in

microprocessors (Motorola MC68701 and MC68705 units), as shown in Figure 4. Thus, the command interface, force-moment and position feedback to the remote support equipment require only a single full duplex RS-232 link. The distributed microprocessors' architecture in the hand uses advanced integrated circuits, including hybrid and high level multifunctional packages, thereby minimizing the chip counts. Custom design circular and annular printed circuit cards support the hand's controller ICs. Seven slip rings interface the local electronics circuits with the central electronics. Four are used for power transmission, two for bidirectional data communication, and the seventh for system ground.

Power for the motor and electronics comes from a support chassis that also houses a National Semiconductor 32016 microprocessor and a Parallax graphics processor for high level control and real-time force-moment graphics display. A control box is used to operate the hand, setting the gripper control mode, changing the give force, rate and position, and adjusting operating parameters such as force and rate limits. This gripper can handle fragile objects with a gentle grasp force of from one to five Newtons, or hold a tool with a firm grip of up to 600 Newtons.

Force and torque gripper control takes place in the hand itself, using a microprocessor for motor control. Commands from the control box are sent to the motor controller via a serial link and the communication processor. On this same route, force, moment and position information is continuously sent to the support chassis for graphic display on a TV monitor. The forces and moments measured by the six-d.o.f. strain gauge force-moment sensor assembly are represented as bar graphs in a star configuration which suggests a perspective view of the Cartesian reference frame of the gripper. Jaw opening and clamping force are represented by vertical bars on the left side of the graphics display. Software provides for two display adjustments; taking away unwanted load bias (like gravity) and scaling the display bars by specifying the force and moment level corresponding to a full bar-graph display. For performance evaluation of this JPL-OMV Smart Hand see Reference 8.

Figure 5 shows a smart hand developed for the Goddard Space Flight Center (GSFC) Flight Telerobotic Servicer (FTS) ground test facility. This hand is also equipped with six-d.o.f. force-torque and one-d.o.f. grasp force sensors. The operation of this smart hand is very similar to the operation of the JPL-OMV hand described above. Note, however, the

reduced volume of electronics of this smart hand and the V-shaped grooves that contour the inner surface of the jaws in two perpendicular directions, as compared to the electronics and to the claw configuration of the JPL-OMV smart hand.

The smart hand shown in Figure 6 was designed at JPL to fit a medium size industrial robot arm such as the PUMA 560. It is used at JPL for research in hybrid motion and force modes of control. The hand has three parts: a jaw mechanism, sensors and local electronics. Powered by a DC torque motor through gears and recirculating ball spindles, the parallel jaw gripper mechanism moves on rails and is supported by linear bearings to minimize friction. Each jaw subassembly consists of three parts: a moving support, a grasp force sensor operating in the range of one to 150 Newtons, and an interchangeable jaw tip. As seen in the photo, V-shaped grooves contour the inner surface of the jaws in two perpendicular directions, assuring a friction-independent, mechanically firm grasp. This permits the gripper to mechanically lock on rectangular or cylindrical objects in two directions with two-d.o.f. constraints or to connect to a T-shaped tool head with three-d.o.f. constraints.

Behind the base of the jaws is a six-axis force-moment sensor with a dynamic range of 75 Newtons and 20 Newton-meters for reading the three orthogonal forces and moments induced by the robot hand's interaction with the environment. This sensor consists of a Maltese cross-like structure instrumented with strain gauges. Strain gauge readings from this sensor are acquired by the local microprocessor, formatted, and transmitted to the central control computer. There, control programs are executed and sensor data are sent to a remote control station.

Local electronics for this smart hand are housed in a shell attached to the force-moment sensor and connected to the robot wrist. In it are two custom printed circuit boards, one for the digital and one for the analog input/output electronics. The digital electronics are based on an Intel 8097 microprocessor with a high number of built-in functions that permit effective management of the real-time multi-tasking environment. The local software system consists of a background process for message analysis and message generation, and an interrupt driven routine for the real-time functions of the controller. The microprocessor clock generates an interrupt every two milliseconds. Presently, three separate grasp control loops are implemented; position,

rate and force controls. When in force control mode, the controller maintains a preset grasp force until the central control computer issues a different command.

More on this smart hand can be found in Reference 9. This hand, called Model A PUMA Smart Hand, is presently being used on one of the PUMA 560 robot arms in the JPL laboratory breadboard system for dual-arm teleoperation described elsewhere in this proceedings. (See Reference 10.)

#### CURRENT SMART HAND DEVELOPMENT AT JPL

The ongoing end effector technology work at JPL is concentrated on the redesign of Model A PUMA Smart Hand to obtain wider dynamic range in task performance both mechanically and electronically. This new design, called Model B and Model C PUMA Smart Hand, contains numerous novelties which fall into two categories: electronic novelties and mechanical novelties.

##### Electronic Novelties

Figure 7 shows Model A and Model B PUMA smart hands side by side. The electronic novelties included in Model B smart hand (and also in Model C smart hand the mechanism of which is described later in this paper) are the following:

- Instead of a conventional design where a microprocessor performs the data collection and communication functions, this new electronics employs a high speed custom designed state machine. This state machine interfaces to a bidirectional fiber optic link for high speed data communication. This circuit achieves a factor of 100 improvement in data collection speed and servo rates up to 10 kHz for a 16 input system. The high servo rate makes it possible to perform advanced signal processing on the force data.
- Due to the high bandwidth of the optical communication link it is not necessary to process the data locally in the hand. All data processing functions are performed at the host processor so all of the software can be written in a familiar and convenient development environment. The software can be changed much more easily.
- In a conventional system the strain gauges are excited by a DC voltage around 5 to 10 volts. The higher this voltage the more signal we get out of the strain gauges with a constant noise level. The voltage is limited by the heat produced in the strain gauges. This voltage is

typically not more than 12 volts. Our new electronics uses a narrow pulse (5  $\mu$ sec wide) to excite the gauges and a very high voltage (100 V). This results a factor of 10 improvement in the signal to noise ratio of the force measurements.

- The above mentioned high strain gauge voltage is variable by software controlling the full scale force range. This method keeps the 12-bit accuracy no matter what force range is used. The control range is a factor of ten, resulting in a virtual floating point force measurement system. The outcome is equivalent to having a 15-bit force reading at 5 kHz rate which can be processed to get a 17-bit value at the system servo rate of 1000 Hz.
- When converting the 8 raw force readings to the 6 Cartesian forces and torques, four of the output numbers are computed as differences of two of the raw readings. If one of the two numbers subtracted reach saturation due to a large force on some other axis, the difference will be inaccurate. To avoid this situation the new circuit subtracts these two numbers in hardware. The result is an accurate Cartesian reading of a small force/torque even if there are large forces acting on other axis. In this arrangement we have 12 raw readings that are converted to 6 Cartesian forces and torques.

According to the block diagram shown in Figure 8, the end effector electronics consists of the following major subsystems:

- PLL clock and state machine
- Power supply
- Motor drive
- A/D converter and input multiplexer
- Sample and hold with preamplifier circuits

The functions of these are as follows:

- The PLL clock and state machine block converts the serial data coming in from the host processor into parallel data bytes and words written to the internal data bus. When all expected bytes have come in, the state machine switches to transmit mode and converts the parallel data coming from the internal bus to a serial bit stream that is transmitted on the output optical fiber to the host processor. The output data also includes the entire received input data as an echo for debugging purposes. This block consists of the following pieces:

- Edge detector
- Packet detector
- Fast clock
- PLL state machine
- Extra bit removal logic
- Serial to parallel conversion logic
- Read/write pulse generation logic
- State change logic

- The function of the edge detector logic is to generate a 10 nanosecond wide pulse every time a positive edge is detected in the data. The packet detector generates a reset signal if there is no input data coming in, removes the reset signal as soon as data begins to come in. The fast clock is an accurate time base for the entire system. This clock runs at 24 MHz, 8 times the bit rate.
- The PLL state machine generates a 3 MHz two-phase clock for data decoding purposes. This clock is phase locked to the pulses coming from the edge detector.
- The extra bit removal logic removes every fifth bit from the incoming data stream. Upon transmission every four bits of data is followed by an extra bit which is added in order to guarantee a level transition that keeps the PLL clock synchronized. These extra bits have to be removed from the receiver data.
- The serial to parallel conversion logic generates the data bus signals from the incoming serial data and it generates the serial outgoing data from the parallel bus signals.
- The read-write pulse generation logic generates a write pulse every time a full byte or word appears on the data bus. This logic supports up to 256 devices on the data bus. When transmission is performed, this logic generates a read pulse for every byte or word to be read into the parallel to serial conversion logic.
- The state change logic counts the incoming data bytes and after a preset number of bytes have come in, it switches to transmit mode. Later when the preset number of bytes have been transmitted, it switches off all circuits and returns to idle mode.

The function of the power supply is to generate the following supply voltages:

+ 5V  
+ 15V  
+ 50V

from a single 30V supply coming into the hand. The +50V supply is not DC but it is a pulse instead. This pulse is emitted every time the hand goes from idle to receive mode and is used to excite the strain gauges. The size of this pulse is under software control. It can be varied from 5 to 50 volts.

The motor drive consists of two identical output circuits. Each one can be software controlled to produce a voltage from -15 to +15 volts. The motor is connected between these two outputs as a bridge. Thus, the motor voltage can vary from 0 to + or - 30 volts.

The A/D converter is a successive approximation 12 bit unit. It performs one conversion in 3 microseconds. The input to this A/D converter is unusual in the sense that the sample and hold circuits are in front of the input multiplexer and so one for each input is needed. This arrangement makes it possible to sample all of the inputs simultaneously, improving the signal quality. This arrangement is also needed because all of the strain gauges are excited with the same pulse. The A/D converter section also includes a standard voltage reference.

Sample and hold with preamplifier circuits. There are 16 input circuits of which 12 are equipped with local D/A converters. These D/A converters are under software control, they are used to remove any offset from the data. Such an offset varies depending on hand orientation, the object grasped and the distance of the grasping from the FT sensor center point. By locally removing these potentially large offsets, the sensitivity of the hand is substantially enhanced. The remaining 4 inputs that do not have D/A converters are used for finger position, motor current and supply voltage sensing.

This hand cannot exist on its own, it always has to be examined in relation to the control processor that it is connected to. The control processor has to be equipped with a matching fiber optic link. This link has been developed to allow our processors to communicate to each other. Currently this link only exists for the Intel ISBX bus of the 32016 within the MULTIBUS environment, but within a few months we are going to make a version for the 68020 in the VME bus environment. The controlling processor outputs a packet to the hand that contains the 16 output commands. Two of these define the motor drive current, the rest specify the bias values for 12 of

the A/D inputs. The hand responds with an echo of these same values followed by the 16 A/D readings, two bytes each. It is up to the control processor to perform the following functions:

- Finger motion control, such as force servicing.
- Signal processing of the input data, such as noise elimination.
- Coordinate transformation of Cartesian forces to task frame.

Although the top speed of the hand is around 10,000 Hz, currently we perform the above functions at a 5000/1000 Hz servo rate. The force readings are taken at 5000 Hz, and the output filtered force data is computed at a 1000 Hz rate.

#### Mechanical Novelties

The latest smart hand mechanical design at JPL is known as the Model C PUMA Smart Hand. This model stands 8.5 inches from its mounting plate to its fingertips and spans just over 7 inches along its widest point (see Figure 9). Physically, the hand attaches to the manipulator arm at the base of a cylindrical bell which houses the four electronic boards described above under Electronic Novelties. Mounted to the upper end of the bell is a force/torque sensor which, in turn, attaches to the mechanism structure. This component houses the motor and drive system to activate the fingers. The two fingers protrude from this structure, being attached via grip force sensors. These fingers, designed to grasp both flat and round objects, are capable of handling up to 3.6 inch objects with a maximum grip force of 60 lbs.

Mechanically, there are three areas that were designed based on the criteria submitted. These are: 1) the overall structural design, 2) the drive mechanism, and 3) the sensing elements. The structural design involved creating a lightweight yet rugged instrument that would take the abuse submitted in a laboratory environment. Designing the drive mechanism consisted of developing a durable, dependable transmission system to actuate the fingers. Sensing design encompasses the detection of loads at the worksite. Each of these will be discussed.

The entire structure of the hand is of anodized aluminum alloy. To create a rugged yet lightweight construction, aluminum 7075-T6 is used since its high strength allows thinner cross-sections. Structurally, the hand is designed to handle a 50 lb external force and 50 ft-lbs of external torque, while only weighing between 4.5 and 5 lbs (total

predicted weight with electronics). Considerable care was taken to shield various delicate components (such as the electronics) from being damaged, but still provide easy access for servicing.

The fingers are actuated by a brushed, direct current, frameless motor (manufactured by Magnetic Technology, capable of 110 oz-in of torque) which directly drives a leadscrew on which the fingers follow. The fingers are supported on Schneeberger crossed-roller linear bearings. To create the opposing motions of the two fingers, the motor was mounted at the center of the leadscrew with right-hand threads extending from one side while left-hand threads are on the other. The result is that the fingers will move in opposite directions for a given motor rotation. This, coupled with the leadscrew's high mechanical advantage, is a very simple and reliable transmission system which provides a compact conversion of the motor's angular motion into the finger's required high-force, linear motion.

Using this type of drive system basically resulted in deciding what type of nut and leadscrew assembly to use, since the losses and mechanical advantage of this assembly dictate the motor size. All of JPL's previous designs which incorporated a leadscrew drive used a ball nut assembly. A ball nut is basically a ball bearing whose races are the screw threads. Such assemblies exhibit very low friction and therefore are highly efficient (greater than 90% as opposed to about 15 to 25% for a bronze nut on a steel leadscrew). Since the efficiency is over 50%, these assemblies are also backdriveable. Three major problems are that ball nut assemblies are susceptible to dirt and debris, require precise alignments, and are very expensive since it would have to be custom-made for this hand (costing about \$5000 per assembly). This led to researching alternative leadscrew designs.

Analyzing the mechanics of leadscrews resulted in four basic design conclusions to improve performance: 1) the screw diameter should be as small as possible, 2) the coefficient of friction between the nut and screw should be below 0.1, 3) the lead angle should be as high as possible (up to 45 degrees), and 4) a square thread should be used as opposed to a acme or "V" thread. Using a square thread increases efficiency and reduces problems caused by dirt because it tends to clean the thread during operation. The first and third conclusions are dependent upon the loading criteria and physical limitations of the hand. The second, though, is primarily a function

of the materials chosen for the nut and leadscrew. Further research found that the coefficient of friction value was the single most contributing factor to having a high efficiency system, as opposed to altering the screw design to reduce frictional effects.

Concentrating the research on various types of low-friction materials, several possible solutions were found for the nut material to operate on a stainless steel leadscrew: 1) Teflon, 2) a solid-film lubricant over a base metal, and 3) Teflon filled Delrin. Teflon is the obvious choice because it has the lowest coefficient of friction of any known solid (about 0.04), but this polymer may have a problem of "creeping" when under a sustained load (while gripping). Literature regarding solid-film lubricants indicated that they may have friction levels comparable to Teflon, but test samples showed this not to be the case (friction about 0.15 to 0.20 at the operating load). DuPont manufactures a Teflon filled Delrin (acetal resin) which would not have the creep problems of the Teflon, but the friction would be twice as high (about 0.08). Overall, Teflon would be the best solution if the creep is acceptable. In the case that Teflon should prove to be unacceptable, a Teflon filled Delrin will be used.

With this drive transmission system, the mechanism would operate at about 55% efficiency with Teflon nuts as opposed to about 40% with the Delrin nuts. Neither system will be backdriveable, even though the Teflon system operates over 50%. This is because the motor's cogging torque is high enough to prevent backdriving at the rated load (60 lbs). This results in a possibly desirable feature. This hand will be capable of gripping an object and maintaining the grip force without continuously supplying power to the motor, yet only incorporate a minimal amount of friction if servoing is required. The accuracy of grip force magnitude after the motor power is discontinued will be a function of the system's and the gripped object's compliance since there will be a slight mechanical relaxation. Although any external loads which are applied may result in undesirable finger forces, this mode could be useful for moving or holding an object in free space with no power dissipation.

Loading and position sensors are essential for completing tasks efficiently. The Model "C" is equipped with three such sensors: 1) finger position sensor, 2) grip force sensor (GFS), and 3) force/torque sensor (FTS). For this hand, it was decided that the finger position did not need to be known very precisely.

Therefore a linear potentiometer is used for this purpose.

To measure the forces applied to the finger, a GFS is used. This sensor is part of the hand's structure which connects the fingers to the mechanism. Any finger force which is applied must be transmitted through this structure, thus causing it to deflect. Semiconductor strain gages are used to detect this deflection and thereby measuring the grip force.

The GFS's shape is that of a rectangular, tubular box (see Figure 10). This design has two key features. Firstly, when under load, the sensor deforms similar to a four-bar linkage, keeping top parallel to the bottom. This results in the faces of the two fingers remaining parallel within a designed tolerance. Secondly, by placing the strain gages in specific locations, the effects of applied moment can be cancelled, thereby measuring only the shear force. The shear force is equal to the grip force whereas the moment is due to where the force is applied on the finger (how far from the sensor). Through a detailed theoretical analysis which was verified by a series of tests, the test location determined for the gages was with all four (full bridge) on the same outer face (see Figure 10). This configuration resulted in the most accurate readings and also provided for the easiest installation.

Between the mechanism and the electronics bell is where the external forces and torques are detected with the FTS. The FTS also uses strain gages, but the structure is much more complex than the GFS. It basically consists of two rigid bodies connected with four beams (see Figure 11). One body attaches to the mechanism while the other to the bell. Therefore any external forces or torques must pass through the beams, resulting in deflections which are detected by 32 strain gages (8 full bridges, 8 gages on each beam). Through the proper decoding scheme, the forces and torque about three orthogonal axes can be determined.

Overall, the Model "C" design has very desirable features for a hand of this nature. It is very rugged in its lightweight, high-strength construction. The actuation system is very simple, incorporating a minimal number of moving parts. Furthermore, the design is very reliable mechanically, which is implied by the simplicity of the transmission system. The Model C smart hand will also be used at the Intelligent Systems Research Lab (ISRL) of Langley Research Center (LaRC).



## CONCLUSION

JPL's smart hands represent only the beginning of the evolutionary trail. Future plans include the addition of new electro-optical proximity and tactile sensing capabilities. Used in close-up work, optical sensors beam infrared light at the object of interest. Reflections from the object's surface will be triangulated to provide depth information. Tactile sensitivity will give robot hands abilities similar to those of human skin, with its sensitivity to touch.

The trend to develop smarter robot hands challenges mechanical design and sensor and microelectronics technology. Hands such as those at JPL were inconceivable just a few years ago, due to the bulk of the local controlling electronics. As circuit size continues to shrink, smart hands will get brighter, bringing increased benefits both in space and on earth.

## ACKNOWLEDGMENTS

The Model A, B and C mechanical design is by Z. Vigh and analysis by T. Ohm. The Model B and C electronics design is by Z. Szakaly. The research described in this paper was performed at the Jet Propulsion Laboratory, California Institute of Technology, under contract with the National Aeronautics and Space Administration.

## REFERENCES

1. Bejczy, A., Jau, B., "Smart Mechanical Hands for Teleoperation in Earth Orbit", Proc. of the 19th Aerospace Mechanisms Symposium, NASA Ames Research Center, May 1-3, 1985.
2. Mishkin, A.H., Jau, B.M., "Space-Based Multifunctional End Effector Systems," JPL Publication 88-16, April 15, 1988.
3. Bejczy, A., "Smart hand - Manipulator Control Through Sensory Feedback", JPL D-107, January 15, 1983.
4. Bejczy, A.K., and Vuskovic, M., "An Interactive Manipulator Control System," Proc. of Second International Symp. on Mini- and Microcomputers in Control, Fort Lauderdale, Fl., Dec. 10-11, 1979.
5. Bejczy, A.K., Brown, J.W., and Lewis, J.L., "Evaluation of Smart Sensor Displays for Multidimensional Precision Control of Space Shuttle Remote Manipulator," Proc. of 16th Annual Conference on Manual Control, MIT, Cambridge, MA., May 5-7, 1980.
6. Bejczy, A.K., and Dotson, R.S., "A Force-Torque Sensing and Display System for Large Robot Arms," Proc. of IEEE Southeastern '82, Destin, Fl., April 4-7, 1982.
7. Bejczy, A.K., Dotson, R.S., Brown, J.W., and Lewis, J.L., "Manual Control of Manipulator Forces and Torques Using Graphic Display," Proc. of IEEE International Conference on Cybernetics and Society, Seattle, WA, Oct. 28-30, 1982.
8. Hannaford, B., "Task-level Testing for the JPL-OMV Smart End Effector", Proceedings of the Workshop on Space Telerobotics, Pasadena, CA, January 30, 1987, JPL Publication 87-13, Vol. 2, pp. 371-380.
9. Fiorini, P., "A Versatile Hand for Manipulators," IEEE Control Systems Magazine, Vol. 8, No. 5, Oct. 1988, pp. 20-24.
10. Bejczy, A.K., Szakaly, Z., and Kim, W.S., "A Laboratory Breadboard System for Dual-Arm Teleoperation," - see elsewhere in this Proceedings.

ORIGINAL PAGE  
BLACK AND WHITE PHOTOGRAPH

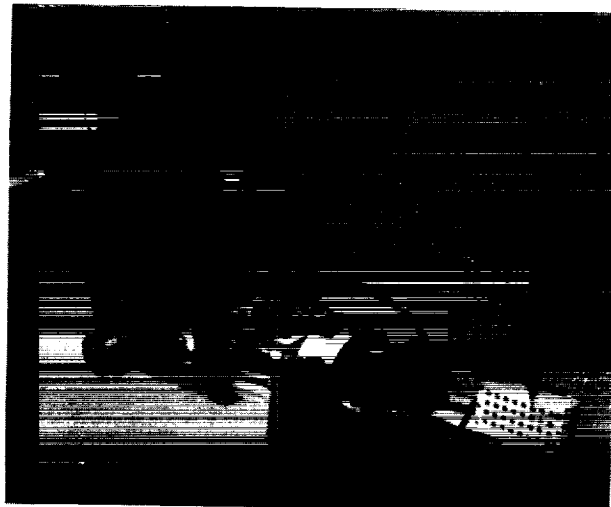
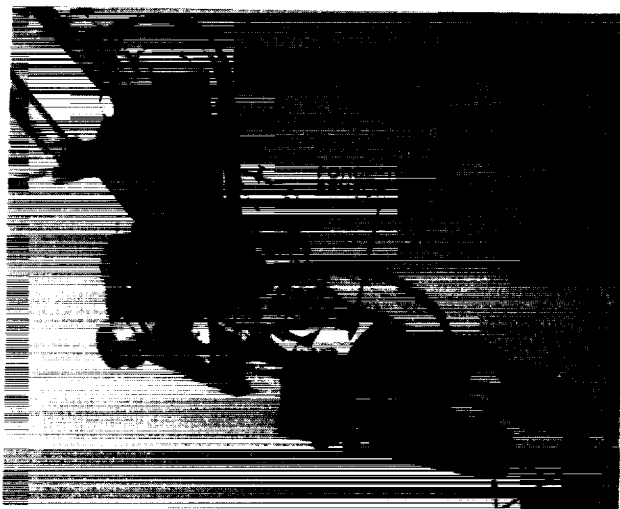


Figure 1. A Smart Hand Early Prototype at JPL (1976-80)

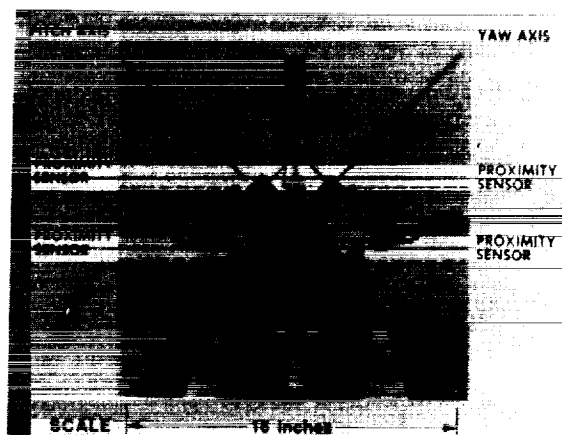


Figure 2. JPL-RMS Smart Hand with Proximity Sensors (1979-81)

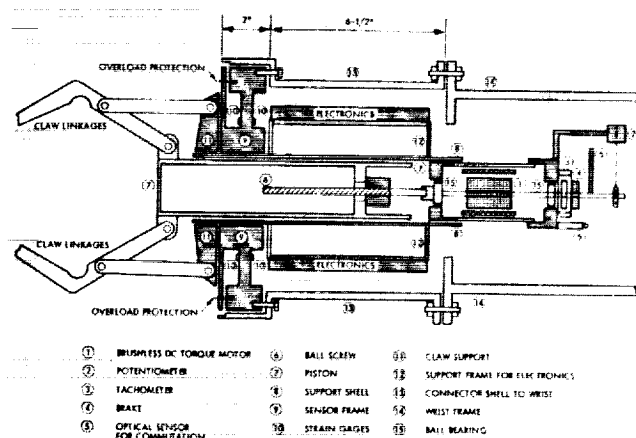


Figure 3. JPL-RMS Smart Hand with Force-Torque Sensor (1982-84)

ORIGINAL PAGE  
BLACK AND WHITE PHOTOGRAPH

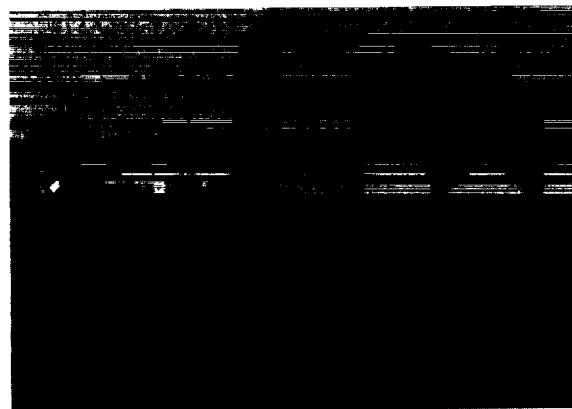
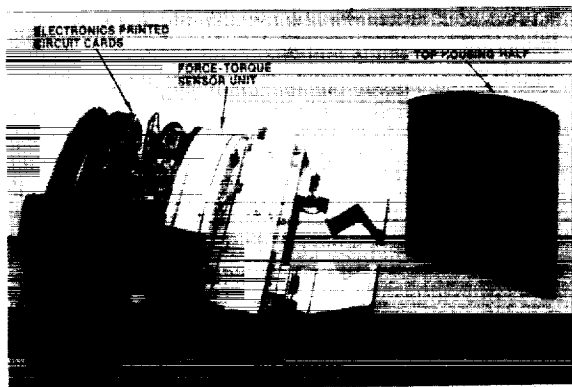
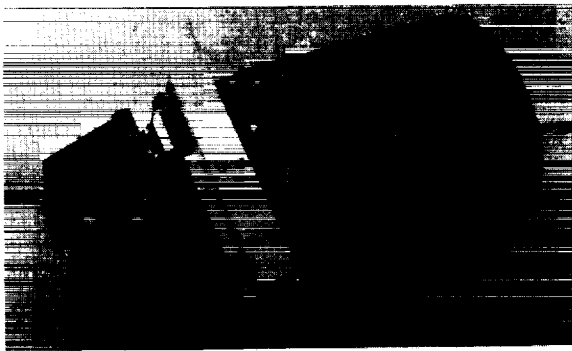


Figure 4. JPL-OMV Smart Hand (1984-86)

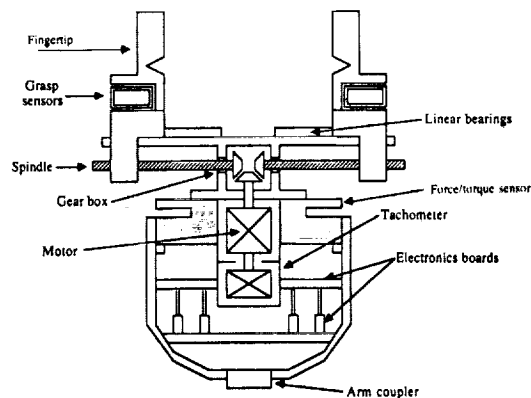
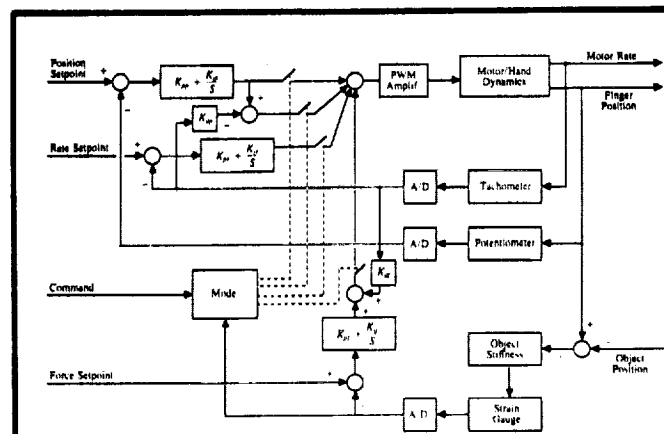


Figure 6. JPL-PUMA 560 Smart Hand and Control, Model A (1988)



Figure 5. JPL-FTS Smart Hand (1987)



ORIGINAL PAGE  
BLACK AND WHITE PHOTOGRAPH

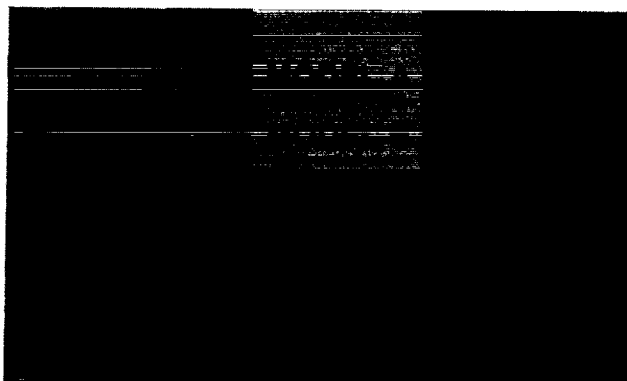


Figure 7. JPL-PUMA 560 Smart Hand Model B (1989)

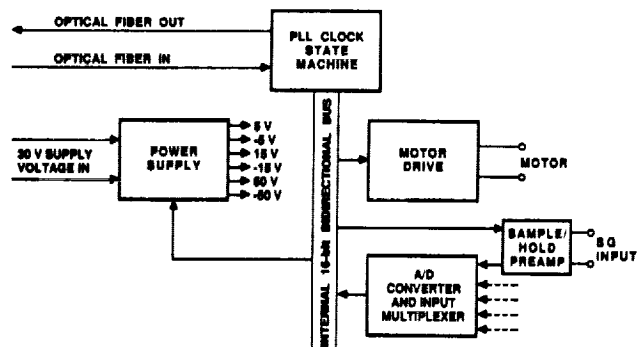


Figure 8. JPL-PUMA 560 Smart Hand Model B and C Electronics Block Diagram (1989)

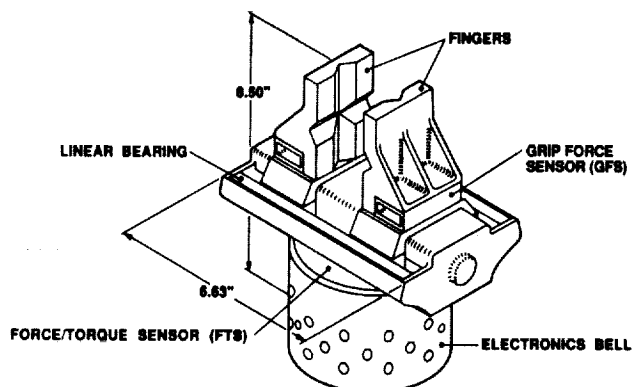


Figure 9. JPL-PUMA Smart Hand Model C Mechanism (1989)

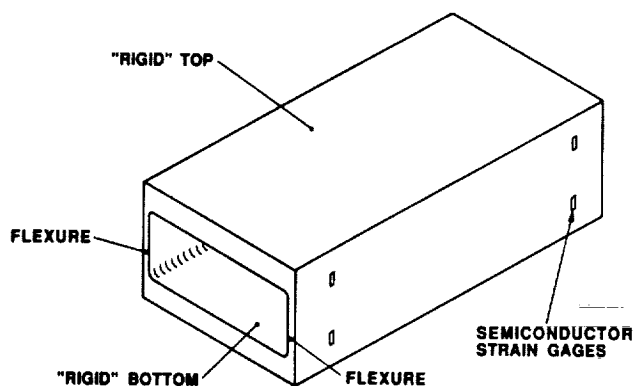


Figure 10. Grip Force Sensor Frame and Gages Schematics

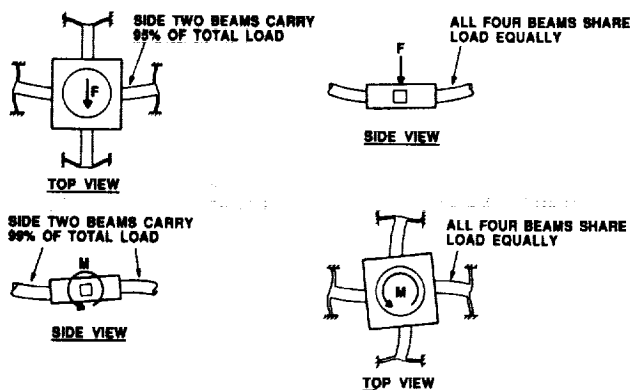
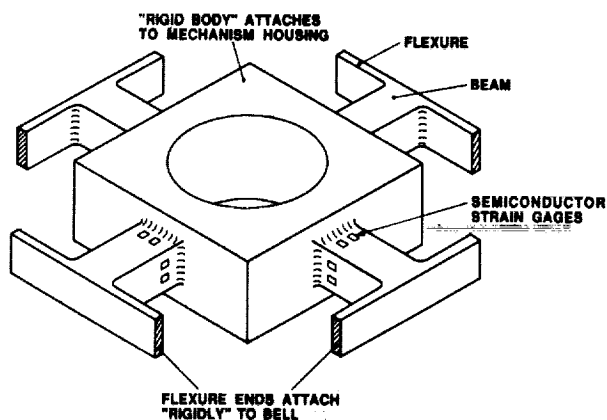


Figure 11. Force-Torque Sensor Frame, Gages and Loading Schematics